Biochimica et Biophysica Acta 1787 (2009) 121–128

Contents lists available at ScienceDirect

Biochimica et Biophysica Acta

journal homepage: www.elsevier.com/locate/bbabio

Towards structural elucidation of eukaryotic photosystem II: Purification, crystallization and preliminary X-ray diffraction analysis of photosystem II from a red alga

Hideyuki Adachi [a], Yasufumi Umena [b], Isao Enami [c], Takahiro Henmi [b], Nobuo Kamiya [b], Jian-Ren Shen [a,*]

[a] Division of Biosciences, Graduate School of Natural Science and Technology, Okayama University, Okayama 700-8530, Japan
[b] Graduate School of Science, Osaka City University, 3-3-138, Sugimoto, Sumiyoshi, Osaka 558-8585, Japan
[c] Department of Biology, Tokyo University of Science, Kagurazaka 1-3, Shinjuku-ku, Tokyo, 162-8601, Japan

ARTICLE INFO

Article history:
Received 2 October 2008
Received in revised form 6 November 2008
Accepted 7 November 2008
Available online 19 November 2008

Keywords:
Photosystem II
Crystallization
Red algae
Cyanidium caldarium
Membrane protein
Dehydration

ABSTRACT

Crystal structure of photosystem II (PSII) has been reported from prokaryotic cyanobacteria but not from any eukaryotes. In the present study, we improved the purification procedure of PSII dimers from an acidophilic, thermophilic red alga *Cyanidium caldarium*, and crystallized them in two forms under different crystallization conditions. One had a space group of $P222_1$ with unit cell constants of $a=146.8$ Å, $b=176.9$ Å, and $c=353.7$ Å, and the other one had a space group of $P2_12_12_1$ with unit cell constants of $a=209.2$ Å, $b=237.5$ Å, and $c=299.8$ Å. The unit cell constants of both crystals and the space group of the first-type crystals are different from those of cyanobacterial crystals, which may reflect the structural differences between the red algal and cyanobacterial PSII, as the former contains a fourth extrinsic protein of 20 kDa. X-ray diffraction data were collected and processed to a 3.8 Å resolution with the first type crystal. For the second type crystal, a post-crystallization treatment of dehydration was employed to improve the resolution, resulting in a diffraction data of 3.5 Å resolution. Analysis of this type of crystal revealed that there are 2 PSII dimers in each asymmetric unit, giving rise to 16 PSII monomers in each unit cell, which contrasts to 4 dimers per unit cell in cyanobacterial crystals. The molecular packing of PSII within the unit cell was constructed with the molecular replacement method and compared with that of the cyanobacterial crystals.

1. Introduction

Photosystem II (PSII) catalyzes a series of light-induced electron transfer reactions, coupled with this is the splitting of water leading to the formation of molecular oxygen which is essential for oxygenic life on the earth. PSII is a multi-pigment protein complex consisting of 17 trans-membrane subunits and 3 peripheral, extrinsic subunits in the case of prokaryotic cyanobacteria [1,2]. The crystal structure of PSII has been reported at resolutions of 3.8–3.0 Å from two species of thermophilic cyanobacteria *Thermosynechococcus elongatus* [3–5] and *T. vulcanus* [6]. These structural studies provided important information on the location and arrangement of various subunits and cofactors within this large membrane-protein complex, and formed the basis for further detailed analysis on the reaction mechanisms taking place in PSII.

The main components of PSII include D1, D2 reaction center subunits, the intrinsic chlorophyll (chl)-binding subunits CP47 and CP43, the α and β subunits of cyt *b*-559, and a number of low molecular mass subunits with single membrane-spanning helix, except PsbZ that has two membrane-spanning helices. These components are largely conserved from prokaryotic cyanobacteria to eukaryotic higher plants. In addition to these membrane-spanning subunits, cyanobacterial PSII contains three extrinsic proteins of 33 kDa (PsbO), 17 kDa (PsbV, cyt *c*-550) and 12 kDa (PsbU) required for maintaining the stability and function of the oxygen-evolving complex (OEC) [7,8]. Among these three extrinsic proteins, PsbO is present in PSII from prokaryotes to eukaryotes. PsbU and PsbV are found in most eukaryotic algae [9,10] but are absent in green algae and higher plants; instead, the functions of PsbU and PsbV are partially replaced by PsbQ and PsbP in green algal and higher plant PSII [11].

Red alga is one of the primitive eukaryotic algae closely related to cyanobacteria. The photosynthetic apparatus of red algae, however, represents an intermediate type between cyanobacteria and higher plants: While PSI of red algae contains chl *a*-binding antenna and thus resembles higher plant PSI [12], PSII of red algae is similar to that of cyanobacteria in that both contain phycobilisome as light-harvesting antenna instead of chl *a*/*b* binding proteins as found in green algae and higher plants. The OEC of red algae also resembles that of

Abbreviations: Chl, chlorophyll; cyt, cytochrome; DDM, n-dodecyl-β-D-maltoside; NCS, non-crystallographic symmetry; OEC, oxygen-evolving complex; PSI, photosystems I; PSII, photosystems II; SDS-PAGE, sodium dodecyl sulfate polyacrylamide gel electrophoresis

* Corresponding author. Fax: +81 86 251 8502.
E-mail address: shen@cc.okayama-u.ac.jp (J.-R. Shen).

0005-2728/$ – see front matter © 2008 Elsevier B.V. All rights reserved.
doi:10.1016/j.bbabio.2008.11.004

cyanobacteria in that it contains PsbU and PsbV [13,14]. There are, however, some apparent differences between PSII of red algae and cyanobacteria: red algal PSII contains a fourth extrinsic protein of 20 kDa (PsbQ′) which is not found in cyanobacterial PSII [13–15]. This protein has a low homology with the PsbQ protein of green algae [15]. In addition, PsbV was found to be able to bind to cyanobacterial PSII independent of other extrinsic proteins [7,16], whereas its binding requires the presence of both PsbO and PsbQ′ in red algal PSII [14]. These differences suggest that some structural differences exist between cyanobacterial and red algal PSII, especially with regard to the lumenal side of PSII.

In order to elucidate the structural differences between cyanobacterial and red algal and other eukaryotic PSII, it is essential to solve the structure of eukaryotic PSII. No reports, however, have been published on the structure of any eukaryotic PSII. Some crystallization trials have been published for higher plant PSII [17–19], but none of the crystals obtained were of sufficient quality for structural analysis. In order to elucidate the structure of red algal PSII and its differences with cyanobacterial PSII, we improved the purification procedure for PSII dimer from an acidophilic, thermophilic red alga *Cyanidium caldarium*. The PSII dimers obtained were then crystallized, and the crystals were characterized by X-ray diffraction analysis.

2. Materials and methods

2.1. Purification of photosystem II

Highly active PSII was purified from *Cyanidium caldarium* based on the procedure of Enami et al. [13] with modifications described below. The cells were suspended in buffer A containing 25% glycerol, 40 mM Mes (pH6.1) and 10 mM $CaCl_2$, to which benzamidine (final concentration of 1 mM), phenylmethylsulfonyl fluoride (final concentration of 1 mM), DNase I and $MgCl_2$ (final concentration of 5 mM) were added. Cells were disrupted by agitation with glass beads of 100 μm in diameter on ice in the dark for 18 cycles; with 10 s on and 4 min off for each cycle. The thylakoid membranes were precipitated by centrifugation at 104,200 ×*g* for 30 min, and the upper part of the precipitants was recovered and re-suspended in buffer A. The thylakoid membranes obtained were solubilized at a chl concentration of 1.2 mg chl/ml with 1.2% n-dodecyl-β-D-maltoside (β-DDM) by stirring in the dark at 0 °C for 40 min. After centrifugation at 104,200 ×*g* for 30 min, the supernatant was filtrated through a 0.4 μm filter and loaded onto a DEAE TOYOPEARL 650 M anion-exchange column equilibrated with 25% glycerol, 40 mM Mes (pH6.1), 3 mM $CaCl_2$ and 0.03% β-DDM. The column was washed with the same buffer containing 0.09 M NaCl until the absorbance of the eluant at 280 nm was decreased to a sufficient low level. Crude PSII particles were then eluted with the same buffer containing 0.23 M NaCl, and the eluate was diluted with a two-fold volume of buffer A, followed by addition of polyethylene glycol 1450 (PEG1450) to a final concentration of 15%. The crude PSII was precipitated by centrifugation, re-suspended in buffer A, and solubilized with a combination of 0.5% β-DDM and 0.7% sucrose monolaurate at a chl concentration of 1.5 mg chl/ml at 0 °C for 20 min. The solubilized, crude PSII was purified with a DEAE TOYOPEARL 650S anion-exchange column with a gradient of 0.05-to-0.15 M NaCl to separate PSII monomers and dimers. The resultant PSII was concentrated by PEG precipitation and suspended in buffer A. Only the dimer fraction was used for crystallization.

2.2. Analysis of protein composition, oxygen-evolving activity, and oligomeric state

Chl concentration was determined according to Ref. [20]. Protein composition of red algal PSII was analyzed using SDS-PAGE with a gradient gel containing 12–20% polyacrylamide and 7.5 M urea [21]. Protein samples were solubilized with 2% (w/v) lithium dodecyl sulfate, 60 mM dithithreitol, and 60 mM Tris–HCl (pH8.5) at 0 °C immediately before electrophoresis. Oxygen evolution of the purified PSII dimer was measured with a Clark-type oxygen electrode at 30 °C under continuous, saturating light in buffer A at a chl concentration of 10 μg/ml. The electron acceptors used were 0.5 mM phenyl-*p*-benzoquinone plus 0.5 mM potassium ferricyanide. The oligomeric

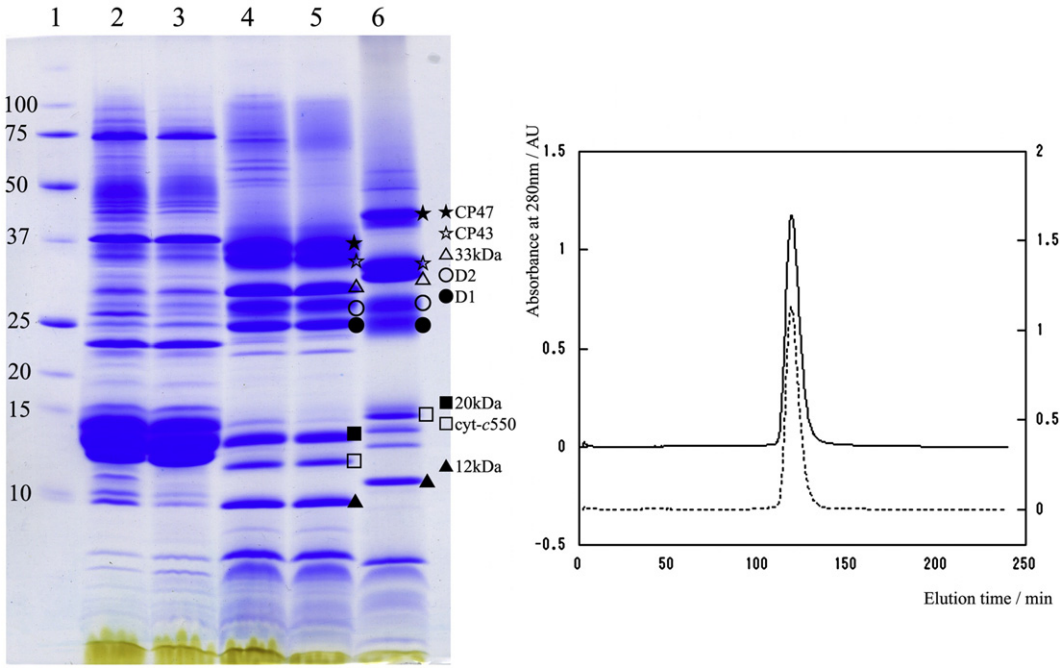

Fig. 1. Analysis of red algal PSII purified from *Cyanidium caldarium*. (A) CBB-stained SDS-PAGE of PSII. Lane 1: molecular mass markers; lane 2: thylakoid membranes (5 μg chl); lane 3: supernatant after β-DDM solubilization (5 μg chl); lane 4, crude PSII (7 μg chl); lane 5: pure PSII dimer (7 μg chl); and lane 6: PSII from the thermophilic cyanobacterium *Thermosynechococcus vulcanus* (7 μg chl). (B) Gel permeation chromatography of PSII dimer from the red alga (solid line) and cyanobacterium (dotted line) using a Superdex 200 PC 3.2/30 column. For other details, see text.

Table 1
Purification yields and oxygen-evolving activities of various samples obtained during each step of the purification from thylakoid membranes of *C. caldarium*

	Yield (%)	Oxygen evolution μmol O_2 /mg chl/hour
Thylakoid membranes	100%	510–1100
β-DDM supernatant	78–100%	672–1020
Crude PSII	7–11%	2346–3710
Pure PSII dimer	4–6%	3000–5000

β-DDM supernatant stands for the supernatant obtained following the first step of β-DDM solubilization prior to column chromatography; crude PSII is the PSII preparation obtained after the first column chromatography, and pure PSII dimer is the final preparation after the second column chromatography. Chl of the starting thylakoid membranes were taken as 100%.

state of PSII was determined by gel filtration chromatography with a column of Superdex 200 PC 3.2/30 equipped to a SMART system (GE Healthcare UK Ltd.) [22]. For comparison, cyanobacterial PSII dimer purified from a thermophilic cyanobacterium *Thermosynechococcus vulcanus* [7,22] was used.

2.3. Crystallization

Crystallization was performed with the method of sitting or hanging drop vapor diffusion. Red algal PSII dimer was precipitated by centrifugation after addition of PEG1450, and re-suspended at 6.0 mg chl/ml in a solution of 5% glycerol, 20 mM Mes (pH6.1), 3 mM $CaCl_2$ containing 0.06% sucrose monocaplate for crystals-1, or 0.05% α-DDM for crystals-2. Crystals-1 were obtained by hanging drop vapor diffusion at 20 °C, with a reservoir solution containing 7.5–8.5% (w/v) PEG1450, 10% glycerol (w/v), 50 mM MES/ sodium succinate-NaOH (pH 5.1), 80 mM LiCl, 10 mM $CaCl_2$ and 0.06% sucrose monocaplate, and a sample solution mixed at a 1:1 ratio of the sample and reservoir solutions. Crystals-2 were obtained by sitting drop vapor diffusion at 4 °C, with a reservoir containing 7–8.0% (w/v) PEG1450, 25% glycerol (w/v), 50 mM MES-NaOH (pH 6.1), 10 mM $CaCl_2$ and 0.05% α-DDM, and a sample mixture with half of the concentration of the reservoir solution.

2.4. X-ray diffraction analysis

For X-ray diffraction measurements, crystals-1 were transferred stepwise to a cryoprotectant solution containing 25% glycerol and 30% (w/v) polyethylene glycol 1450, 50 mM MES/ sodium succinate -NaOH (pH5.1), 80 mM LiCl, 10 mM $CaCl_2$ and 0.06% sucrose monocaplate, and flash-frozen in a nitrogen gas stream at 100K. Crystals-2 were transferred to 35% (w/v) PEG2000 and 12% glycerol by dialysis for 4 days at 4 °C. X-ray diffraction experiments were performed at BL41XU of SPring-8, Japan [23], using a CCD detector Quantum 315 (ADSC) or Mar 225 (Mar Research) at 100K. The X-ray wavelength and sample-to-detector distance were 1.0 Å and 500 mm, respectively. An oscillation angle of 0.6° and an exposure time of 4 s were applied for each of 300 frames. X-ray diffraction data were processed with HKL2000 [24].

Self-rotation functions were calculated with the Polarrfn program in CCP4 [25] using data sets of crystal-2 and cyanobacterial PSII crystal in the resolution range of 15–5 Å, with an integration radius of 20 Å. Molecular packing in the crystal-2 was determined with the molecular replacement method with the CNS program [26]. Cyanobacterial PSII monomer structure containing 4 intrinsic subunits (D1, D2, CP43, and CP47) and 3 extrinsic subunits (33 kDa, cytochrome *c*-550 and 12 kDa) (PDB code: 2AXT) was used as the initial search-model, since these 7 large subunits are commonly present in cyanobacterial and red algal PSII, and appeared to be needed for determining the rotation function in the molecular replacement calculation. All residues of the search-model were exchanged to alanine and all prosthetic molecules were excluded. We searched the structure of one of the two dimers in the asymmetric unit in which, the position of one monomer was initially determined and then the position of the other monomer was searched based on the cyanobacterial PSII structure to complete the dimer structure. The structure of the other dimer was subsequently searched using the dimer structure previously determined as the next search model. The position of each monomer was roughly refined with rigid body refinement using the CNS program.

3. Results

3.1. Purification of PSII dimer from the red alga C. caldarium

PSII from *C. caldarium* has been purified previously using one step of anion exchange column chromatography [13,14]. We initially tried to crystallize PSII purified based on the previous procedure, which was proved unsuccessful due to a mixture of PSII monomer and PSII dimer as well as some other minor contamination from non-PSII components. We therefore improved the purification procedure by using two steps, instead of one step, of anion exchange column to separate PSII dimer from monomer and other contaminating components. We first used a strong anion-exchange column (High Performance Q-sepharose, GE Healthcare UK Ltd.) for the second step of column purification, which yielded a highly purified PSII dimer. However, the extrinsic 20 kDa protein was found to be largely dissociated from the purified PSII, suggesting its weak association with PSII. Therefore, we employed a DEAE TOYOPEARL 650S anion-exchange column for the second step purification, which yielded a highly purified, active PSII dimer preparation retaining the 20 kDa protein. The resultant PSII preparation was analyzed by SDS-PAGE and gel filtration chromatography (Fig. 1). The SDS-PAGE pattern shows that all major PSII subunits are retained, and the subunit composition of red algal PSII is similar to that of cyanobacterial PSII, except for the presence of the 20 kDa extrinsic protein in the red algal PSII as well as some differences in the

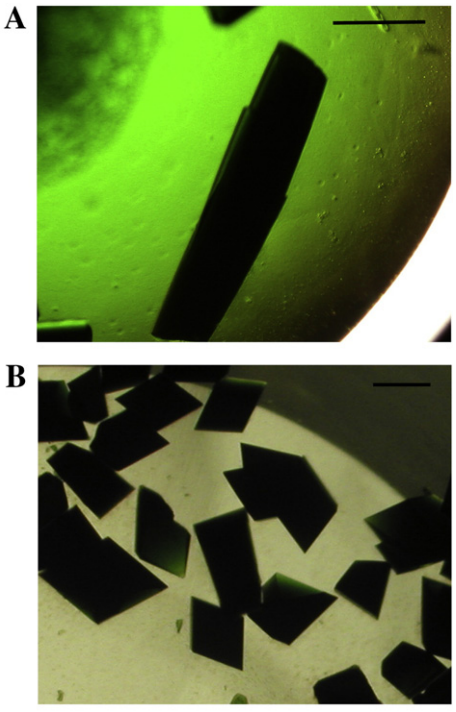

Fig. 2. Crystals of different shape and sizes of the PSII dimer complex from the red alga *Cyanidium caldarium*. (A) Rod-shaped crystals (crystal-1) grown by the hanging drop vapor diffusion method. (B) Rhombic crystals (crystal-2) grown by the sitting drop vapor diffusion method at 277K. The bar represents 0.2 mm in both of the panels.

mobilities of most of the large subunits between the two organisms. Gel filtration chromatography showed that the purified red algal PSII gave rise to a single peak, indicating that it is homogeneous in terms of its size. The elution peak was in the same position as that of cyanobacterial PSII dimer [22], indicating that the red algal PSII obtained is also a dimer.

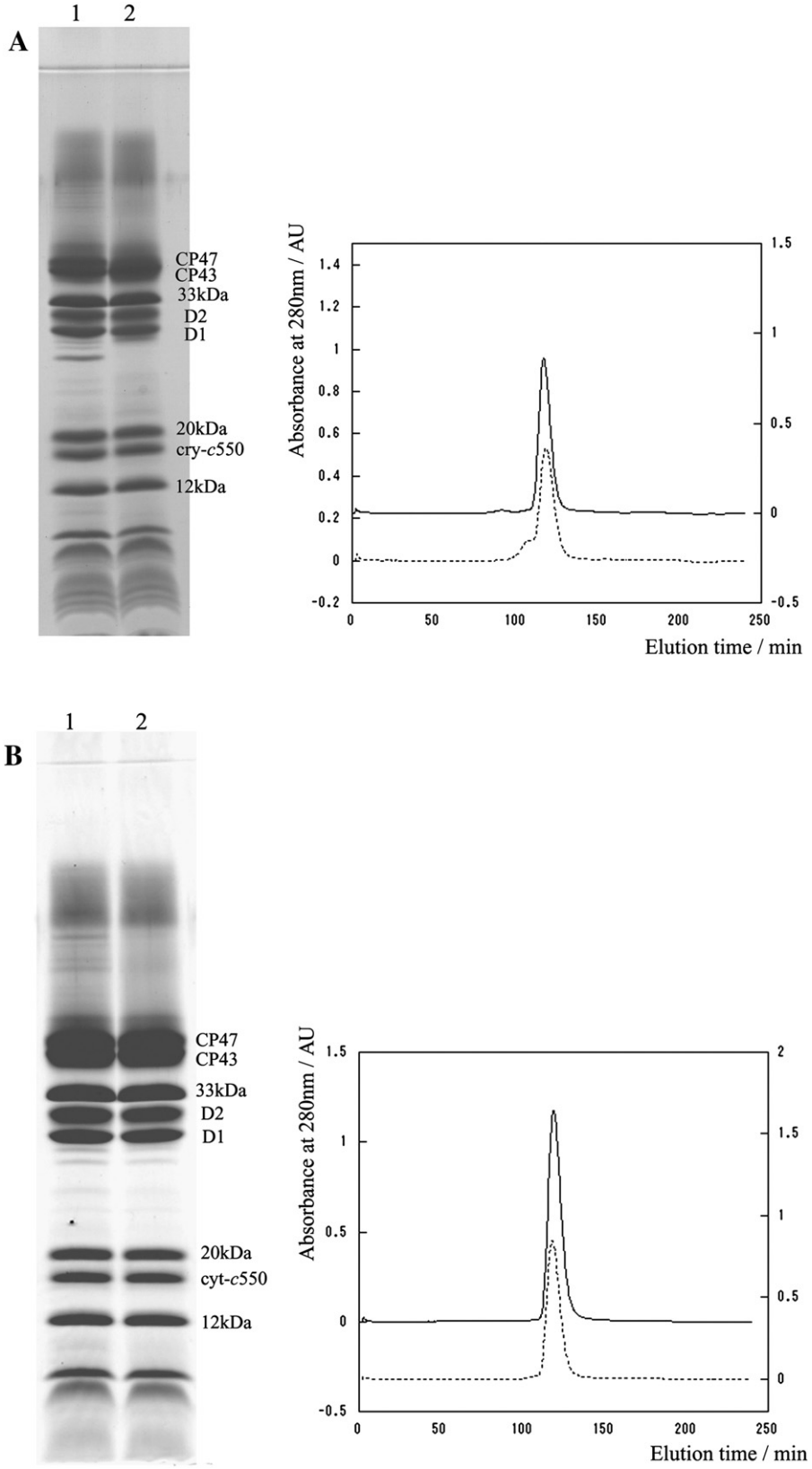

Fig. 3. Analysis of red algal PSII before and after crystallization. Left: SDS-PAGE patterns of dimeric PSII before crystallization (lane 1), and after crystallization (re-dissolved crystals) (lane 2). Right: gel filtration chromatography patterns of PSII before crystallization (dashed lines) and after crystallization (re-dissolved crystals) (solid lines). A: crystals-1; B: crystals-2.

Table 1 shows the oxygen-evolving activities and recovery of chl of various samples obtained in each purification step. The final PSII dimer has a yield of 4–6% based on the amounts of chl in the starting material of thylakoids, and its oxygen-evolving activity ranges from 3000-to-4000 μmol O_2 per mg chl per hour. This activity is comparable to the PSII dimer obtained from thermophilic cyanobacteria [7,22,27] but much higher than PSII from most of other eukaryotic organisms which typically has an oxygen-evolving activity of around 1000 μmol O_2 per mg chl per hour [28–32].

3.2. Crystallization

Initial crystallization trials were carried out employing similar conditions used for crystallizing cyanobacterial PSII dimer [4–6,22,27,33]. However, this yielded no crystals from the red algal PSII dimer. The crystallization conditions were thus screened and determined as described in Materials and methods, which yielded two different types of crystals for the purified red algal PSII dimer (Fig. 2). Rod-shaped crystals (designated as crystals-1) were grown by the hanging drop vapor diffusion method in 7–10 days at 20 °C; they grew to a maximum size of 1.0 mm×0.2 mm×0.2 mm (Fig. 2A). On the other hand, rhombic-shaped crystals (designated as crystals-2) were grown by the sitting drop vapor diffusion method under slightly different conditions, and they grew to a maximum size of 0.5 mm×0.4 mm×0.2 mm at 4 °C (Fig. 2B).

The subunit composition and oligomeric state of PSII in the two types of crystals were analyzed by SDS-PAGE and gel filtration after re-dissolving the crystals, and compared with PSII before crystallization. As Fig. 3 shows, the subunit composition of PSII in both crystals is essentially the same as that before crystallization, except the absence of some faint bands in the crystals that were otherwise present before crystallization, indicating the incorporation of only PSII components into the crystals. The elution time from the gel filtration column was also exactly the same for PSII before and after crystallization (Fig. 3), indicating that the red algal PSII retained its dimeric structure in both crystals.

3.3. X-ray diffraction analysis

The properties of red algal PSII crystals were analyzed with X-rays from a synchrotron radiation facility SPring-8, Japan [23]. A typical image of the diffraction pattern from the crystals-1 was shown in Fig. 4A, which showed that it diffracted to a maximum resolution of 3.8 Å. A full data set was collected and processed to a resolution of 3.8 Å (Table 2), which showed that this crystal belongs to the orthorhombic space group $P222_1$, with unit cell constants of a=146.8 Å, b=176.9 Å, and c=353.7 Å, respectively. These indicate that the crystals-1 had a different space group and unit cell constants with that of cyanobacterial PSII. The unit cell volume of crystals-1, however, was calculated to be 9.19×10^6 Å^3, which is similar to that of the cyanobacterial crystals.

When the crystals-2 were transferred to the cryoprotectant solution in a stepwise way similar to that used for crystals-1, the crystals diffracted to a resolution of 8.0–9.0 Å (data not shown). Processing of several images collected at different angles from the crystal gave rise to approximate unit cell constants of a=224 Å,

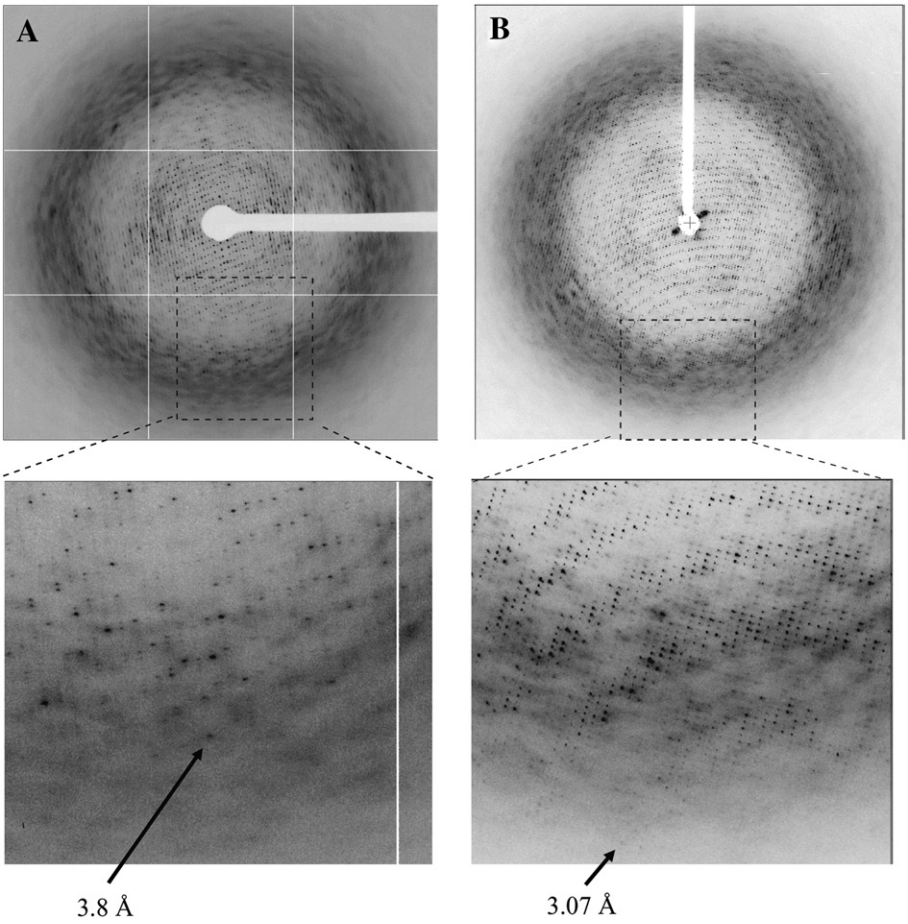

Fig. 4. Diffraction patterns of red algal PSII crystals taken at BL41XU of SPring-8, Japan, using a CCD detector. The X-ray wavelength and the sample-to-detector distance were 1.0 Å and 500 mm, respectively. The crystal was frozen at 100K under a cooled nitrogen gas stream. An oscillation angle of 0.6° and an exposure time of 4 sec were applied for each frame. (A) Diffraction pattern from a crystal-1; (B) diffraction pattern from a crystal-2. Lower panels represent the enlarged view of the boxed area in the upper panels of both A and B.

Table 2
Statistics of X-ray diffraction data collected from the two types of red algal PSII crystals, and their space group and unit cell parameters

Data set	Crystal-1	Crystal-2	
X-ray source	BL41XU	BL41XU	
Resolution/Å	50–3.8	50–3.5	
Unique reflections	84400	194038	
Redundancy	6.7 (6.7)	7.4(7.3)	
Rmerge (%)	8.0 (78.0)	10.5(75.9)	
$I/\sigma(I)$	19.6 (1.95)	21.7(2.15)	
Completeness (%)	91.0 (86.1)	99.9(100.0)	
			Cyanobacterial PSII[a]
Space groups	$P222_1$	$P2_12_12_1$	$P2_12_12_1$
Unit cell dimensions (Å)	a=146.8	a=209.2	a=126.5
	b=176.9	b=237.5	b=222.4
	c=352.7	c=299.8	c=303.3
Unit cell volumes (Å^3)	9.19×10^6	1.49×10^7	8.53×10^6
Solvent content (%)	62.5	56.0	66.0
V_M[b]	3.3	2.8	3.6
Z[b]	8	16	8

[a] For comparison the space group and unit cell parameters of cyanobacterial PSII were also listed [6, 22].
[b] V_M: the Matthews coefficient (Å^3/Da); Z: number of monomer in the unit cell.

b=264 Å, and c=326 Å, although we did not collect the full data set from the crystals due to its low resolution. This yields a unit cell volume of 1.93×10^7 Å^3, which is more than double of that of crystals-1 or cyanobacterial crystals. This suggested that the lower resolution of crystals-2 might be due to its too large solvent content, resulting in a too loose packing of PSII dimers within the unit cells. In order to improve the resolution, we employed a dehydration procedure by which, the crystallization solution was changed to the final cryoprotectant solution gradually through dialysis for 4 days. This procedure improved the resolution dramatically, and yielded a diffraction pattern with a maximum resolution of 3.07 Å (Fig. 4B). A full data set was collected and processed to a resolution of 3.5 Å, which showed that this type of crystal belongs to the orthorhombic space group $P2_12_12_1$. This space group is the same as that of the cyanobacterial crystals but different from that of crystals-1. The unit cell constants of crystals-2 after dehydration were determined to be a=209.2 Å, b=237.5 Å, and c=299.8 Å, respectively (Table 2), which yielded a unit cell volume of 1.49×10^7 Å^3. This unit cell volume is 23% less than that before dehydration, indicating a significantly compact arrangement of PSII dimers within the crystals.

3.4. Molecular packing of crystal-2

Based on the unit cell volume and molecular mass of cyanobacterial PSII monomer, the Matthews coefficient of the red algal crystals-2 was calculated to be 2.8 Å^3 Da^{-1} if we assume that there are 16 PSII monomers within a unit cell, suggesting the presence of 4 monomers in an asymmetric unit. This gives rise to a solvent content of 56% (Table 2). Since PSII used for crystallization exists as a dimer, these results suggest that 2 dimers were included in an asymmetric unit, in other words, each asymmetric unit is composed of a PSII tetramer. This is supported by the self-rotation function calculated from the red algal crystals-2. As depicted in Fig. 5A, the self-rotation function of crystals-2 showed peaks at κ=180° section, indicating the presence of a two-fold axis as non-crystallographic symmetry (NCS) around polar angles of ω=45°, φ=0°. When the PSII tetramer has a non-crystallographic 222 symmetry and the second two-fold axis is roughly parallel to the b-axis, the third two-fold axis will also appear around ω=45°, φ=0° because of the *mmm* symmetry of rotation function for the space group $P2_12_12_1$. Thus, the second and third two-fold axis were not clearly separated in the rotation function obtained, which is in line with the assumption that a PSII tetramer is included in the asymmetric unit.

For comparison, the self-rotation function of a cyanobacterial PSII crystal was shown in Fig. 5B. A typical peak was found around ω=45°, φ=90° in the κ=180° section. The two rotation functions of red algal and cyanobacterial PSII crystals are very similar with each other, except that the NCS two-fold axis exists in the *ac*-plane in the former but in the *bc*-plane in the latter, and the peak height in Fig. 5A is roughly double of that in Fig. 5B. The unit cell constants a, b, and c of red algal crystals-2 (Table 2) corresponded to those of b, twice of a, and c of the cyanobacterial PSII crystals, respectively. These findings suggest that the molecular packing of PSII dimers in red algal crystal is similar with that in the two adjacent unit cells of b, $2a$, and c of the cyanobacterial PSII crystals. The difference is that the tetramer in the red algal crystal has a non-crystallographic 222 symmetry, whereas the dimer in cyanobacterial PSII crystal has only a non-crystallographic two-fold symmetry.

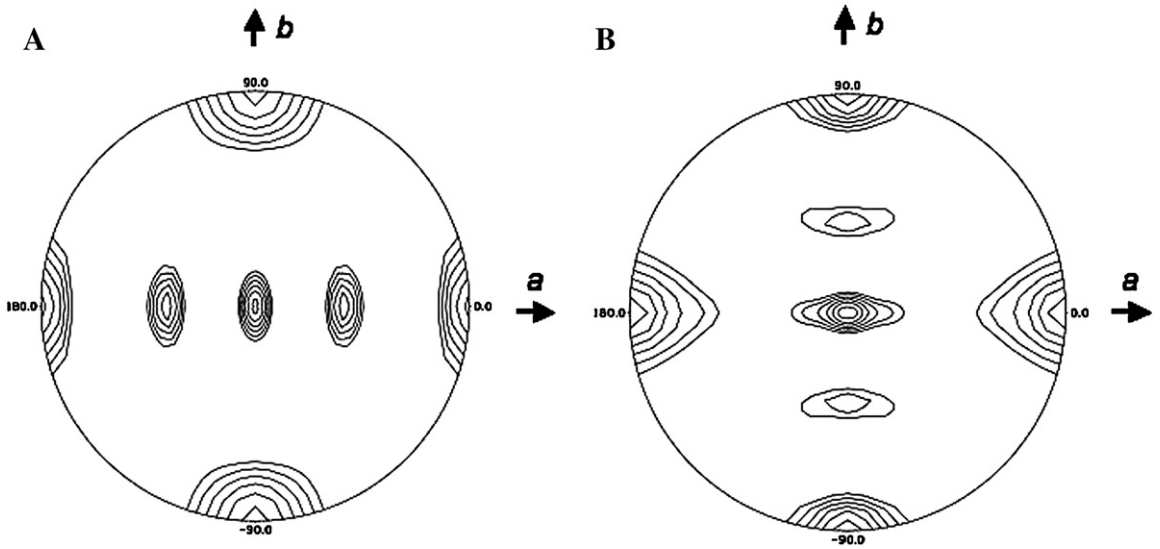

Fig. 5. Self-rotation functions of a red algal crystal-2 (A) and a cyanobacterial crystal (B). The functions were calculated in the resolution range of 5–15 Å at a radius of integration of 20 Å using Polarrfn program in the CCP4 program suit [25]. The peaks represent two-fold axis in the κ=180° section. The directions are defined in polar angle by omega (angle from the c-axis) and phi (angle from the a-axis in the ab-plane). The peak heights corresponding to crystallographic two-fold axis was normalized to 1.0 and contours were drawn from 0.4 with 0.1 steps.

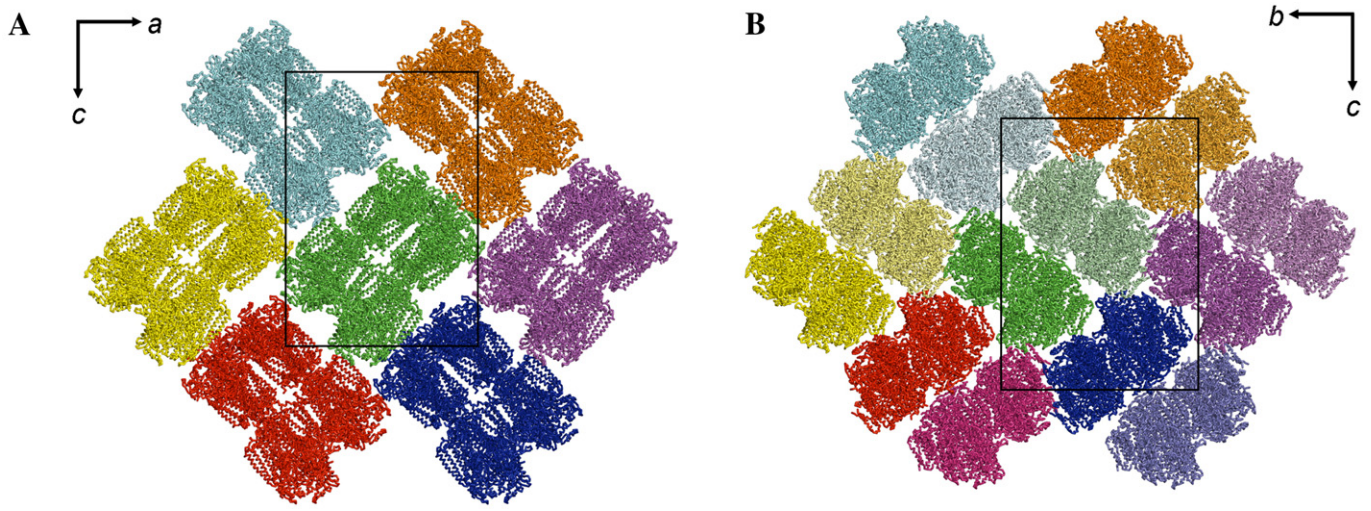

Fig. 6. Molecular arrangement of PSII in unit cells of red algal crystal-2 (A) and cyanobacterial PSII crystals (B). The area surrounded by the black frame indicates a unit cell. For clarity, one of the two layers in the unit cell of red algal crystal-2 (A) was omitted.

In order to determine the real molecular arrangement in the unit cells of red algal crystals-2, we used the molecular replacement method to analyze the red algal PSII structure using the cyanobacterial structure [5] as the search model. The structure of PSII thus determined showed a tetrameric form which is arranged as a dimer-of-dimer (Fig. 6). Each PSII tetramer was formed by stacking of two PSII dimers at the surface of their stromal side, where no large protrusions were found out of the membrane. The tetramers form a series of stacked planes relative to the NCS two-fold axis perpendicular to the *ac*-plane (Fig. 6A). The adjacent tetramers are rotated by about 90° with respect to each other. For comparison, the molecular arrangement of PSII dimer in cyanobacterial crystals was shown in Fig. 6B. It appears that one of the two layers in the unit cell of the red algal crystals-2 is achieved by small rotational (5–10°) and translational shifts of the cyanobacterial PSII dimers, and stacking of the two layers yielded 4 monomers in an asymmetric unit in the red algal crystal. The small rotations coincide with the fact that the peaks observed in the rotation function of cyanobacterial PSII crystal were distributed in a similar range with that of the red algal crystal (Fig. 5).

4. Discussion

Although the central part of PSII is highly conserved from cyanobacteria to higher plants, there exist important differences in the subunit composition of OEC among various organisms. In order to elucidate these structural differences as well as the evolutionary changes of PSII, it is essential to solve its crystal structure from various eukaryotic photosynthetic organisms. Here we purified the PSII dimer from the eukaryotic red alga *C. caldarium*, and succeeded in its crystallization. An active PSII preparation has been obtained from this red alga previously [13,14]. However, that PSII preparation was found unsuitable for crystallization, since it was a mixture of PSII monomer and dimer, and also contained minor contaminations from some non-PSII components. We extended the previous purification procedure by introducing a second column step, which successfully separated PSII monomer and other contaminating components from the PSII dimer. The resultant PSII dimer had a very high oxygen-evolving activity comparable to those of thermophilic cyanobacterial PSII. This was achieved by inclusion of glycerol in the media for column chromatography. As a matter of fact, when no glycerol was included in the column buffer, we found that the oxygen-evolving activity was reduced to 1720–710 μmol O_2 per mg chl per hour.

While a high oxygen-evolving activity is important for obtaining good-quality crystals, another factor that turned to be important was found to be the detergents used to solubilize PSII before the second column chromatography. If the second column chromatography was carried out in a similar way as the first step of column purification, e.g., PSII sample was solubilized with only β-DDM prior to the second column chromatography, the resultant PSII dimer was highly pure and active in terms of analysis by SDS-PAGE, gel electrophoresis, and oxygen-evolving activity. However, this dimer preparation tended to aggregate easily and thus yielded low quality crystals despite an extensive search for the crystallization conditions (data not shown). After searching for detergents suitable for solubilization prior to the second column purification, we found that a combination of β-DDM *plus* sucrose monolaurate gave rise to a PSII dimer that is hardly aggregated. After searching for the crystallization conditions, this PSII dimer gave rise to the best crystals as described in the Results section.

By using different crystallization methods and conditions, we obtained two types of crystals from the red algal PSII dimer. Crystals-1 had a space group of $P222_1$ which is different from that of cyanobacterial PSII. Its unit cell constants were also different from that of cyanobacterial PSII. The unit cell volume of crystals-1, however, was similar to that of cyanobacterial PSII, suggesting that they contain the same number of PSII dimer in each unit cell which has been determined to be four in the cyanobacterial PSII crystals.

Crystals-2 had the same space group of $P2_12_12_1$ as that of cyanobacterial PSII. Its unit cell constants, however, were significantly larger than that of cyanobacterial PSII even after the dehydration-treatment, resulting in a much larger unit cell volume. As a result, the number of PSII monomers in each unit cell was determined to be 16, and they form tetramers in the crystals. Since the red algal PSII used for crystallization exists as a dimer, and also since re-dissolved crystals showed only the dimeric form of PSII, it was concluded that PSII dimers either joined together to form the PSII tetramer under the crystallization conditions, or were re-arranged to the tetrameric form within the crystals by the dehydration treatment.

The different behavior observed between red algal and cyanobacterial PSII may reflect the differences in the composition of extrinsic proteins between the red algae and cyanobacteria, as the former contain an extra 20 kDa extrinsic protein. It is known that the hydrophilic surfaces usually play important roles in forming the molecular contact for membrane proteins, and indeed, the extrinsic proteins were found to constitute the major crystal contacts in the case of cyanobacterial PSII crystals [4–6]. The presence of the 20 kDa protein in red algal PSII may therefore affect the molecular packing of the red algal crystals.

The resolution of crystals-2 was increased significantly by the post-crystallization dehydration procedure. This is supported by the reduction in the unit cell constants and the solvent content after dehydration. In fact, the solvent content of red algal crystal after dehydration is 10% lower than that of the cyanobacterial PSII crystals [22]. Improvement of resolution by means of dehydration has been reported for a number of soluble protein crystals, whereas not many examples have been reported for membrane protein crystals. The present results thus present another example for improving crystal quality of membrane protein complexes by post-crystallization dehydration [34,35].

In conclusion, we improved the purification procedure for PSII from the red alga *C. caldarium*, which yielded a highly purified PSII dimer with a high oxygen-evolving activity comparable with that of thermophilic cyanobacterial PSII. We obtained two types of crystals from the red algal PSII dimer under slightly different conditions, and obtained X-ray diffraction data with resolutions suitable for structure analysis. Crystals-1 had a different space group and unit cell constants with cyanobacterial PSII crystals, whereas crystals-2 had the same space group but different unit cell constants and unit cell volume as that of cyanobacterial crystals. All these may reflect the structural differences between the red algal and cyanobacterial PSII. The crystals obtained in the present study will allow us to analyze the structure of red algal PSII.

Acknowledgements

We thank the beamline scientists at BL41XU of SPring-8 for their help on the X-ray diffraction experiments. This work was supported by a Grant-in-Aid for Scientific Research on Priority Areas (Structures of Biological Macromolecular Assemblies), a Grant-in-Aid for Creative Scientific Research, a Grant-in-Aid for Scientific Research (20570038), and a GCOE program from the Ministry of Education, Culture, Sports, Science and Technology of Japan.

References

[1] F. Müh, T. Renger, A. Zouni, Crystal structure of cyanobacterial photosystemII at 3.0 Å resolution: a closer look at the antenna system and the small membrane-intrinsic subunits, Plant Physiol. Biochem. 46 (2008) 238–264.
[2] J.R. Shen, T. Henmi, N. Kamiya, Structure and function of photosystem II, in: F. Fromme (Ed.), Photosynthetic Protein Complexes, A Structural Approach, WILEY-VCH, 2008, pp. 83–106.
[3] A. Zouni, H.T. Witt, J. Kern, P. Fromme, N. Krauss, W. Saenger, P. Orth, Crystal structure of photosystem II from *Synechococcus elongatus* at 3.8 Å resolution, Nature 409 (2001) 739–743.
[4] K.N. Ferreira, T.M. Iverson, K. Maghlaoui, J. Barber, S. Iwata, Architecture of the photosynthetic oxygen-evolving center, Science 303 (2004) 1831–1838.
[5] B. Loll, J. Kern, A. Zouni, W. Saenger, J. Biesiadka, K.D. Irrgang, Towards complete cofactor arrangement in the 3.0 Å resolution structure of photosystem II, Nature 438 (2005) 1040–1044.
[6] N. Kamiya, J.-R. Shen, Crystal structure of oxygen-evolving photosystem II from *Thermosynechococcus vulcanus* at 3.7-Å resolution, Proc. Natl. Acad. Sci. U. S. A. 100 (2003) 98–103.
[7] J.-R. Shen, Y. Inoue, Binding and functional properties of two new extrinsic components, cytochrome *c*550 and a 12 kDa protein, in cyanobacterial photosystem II, Biochemistry 32 (1993) 1825–1832.
[8] J.-R. Shen, M. Qian, Y. Inoue, R.L. Burnap, Functional characterization of *Synechocystis* sp. PCC 6803 Δ*psb*U and Δ*psb*V mutants reveals important roles of cytochrome *c*-550 in cyanobacterial PSII, Biochemistry 37 (1998) 1551–1558.
[9] I. Enami, S. Yoshihara, A. Tohri, A. Okumurata, H. Ohta, J.-R. Shen, Cross-reconstitution of various extrinsic proteins and photosystem II complexes from cyanobacteria, red alga and higher plant, Plant Cell Physiol. 41 (2000) 1354–1364.
[10] I. Enami, T. Suzuki, O. Tada, Y. Nakada, K. Nakamura, A. Tohri, H. Ohta, I. Inoue, J.R. Shen, Distribution of the extrinsic proteins as a potential marker for the evolution of photosynthetic oxygen-evolving photosystem II, FEBS J. 272 (2005) 5020–5030.
[11] J.L. Roose, K.M. Wegener, H.B. Pakrasi, The extrinsic proteins of photosystem II, Photosynth. Res. 92 (2007) 369–387.
[12] G. Wolfe, F.X. Cunningham, D. Durnford, B. Green, E. Gantt, Evidence for a common origin of chloroplasts with light-harvesting complexes of different pigmentation, Nature 367 (1994) 566–568.
[13] I. Enami, H. Murayama, H. Ohta, M. Kamo, K. Nakazato, J.-R. Shen, Isolation and characterization of a photosystem II complex from the red alga *Cyanidium caldarium*: association of cytochrome *c*-550 and a 12 kDa protein with the complex, Biochim. Biophys. Acta 1232 (1995) 208–216.
[14] I. Enami, S. Kikuchi, T. Fukuda, H. Ohta, J.-R. Shen, Binding and functional properties of four extrinsic proteins of photosystem II from a red alga, *Cyanidium caldarium*, as studied by release-reconstitution experiments, Biochemistry 37 (1998) 2787–2793.
[15] H. Ohta, T. Suzuki, M. Ueno, A. Okumura, S. Yoshihara, J.-R. Shen, I. Enami, Extrinsic proteins of photosystem II: an intermediate member of PsbQ protein family in red algal PS II, Eur. J. Biochem. 270 (2003) 4156–4163.
[16] J.-R. Shen, R.L. Burnap, Y. Inoue, An independent role of cytochrome *c*-550 in cyanobacterial photosystem II as revealed by double-deletion mutagenesis of the *psbO* and *psbV* genes in *Synechocystis* sp. PCC 6803, Biochemistry 34 (1995) 12661–12668.
[17] C. Fotinou, M. Kokkinidis, G. Fritzsch, W. Haase, H. Michel, D.F. Ghanotakis, Characterization of a photosystem-II core and its 3-D crystals, Photosynth. Res. 37 (1993) 41–48.
[18] J.-R. Shen, N. Kamiya, 3D crystal structure of the photosystem II core, in: T.J. Wydrzynski, K. Satoh (Eds.), Photosystem II: The Light-Driven Water:Plastoquinone Oxidoreductase, Springer, The Netherlands, 2005, pp. 449–467.
[19] I.K. Smatanová, J.A. Gavira, P. Rezácová, F. Vácha, J.M. García-Ruiz, New techniques for membrane protein crystallization tested on photosystem II core complex of *Pisum sativum*, Photosynth. Res. 90 (2007) 255–259.
[20] R.J. Porra, W.A. Thompson, P.E. Kriedemann, Determination of accurate extinction coefficients and simultaneous equations for assaying chlorophylls *a* and *b* extracted with four different solvents: verification of the concentration of chlorophyll standards by atomic absorption spectrometry, Biochim. Biophys. Acta 975 (1989) 384–394.
[21] M. Ikeuchi, Y. Inoue, A new photosystem II reaction center component (4.8 kDa protein) encoded by chloroplast genome, FEBS Lett. 241 (1988) 99–104.
[22] J.-R. Shen, N. Kamiya, Crystallization and the crystal properties of the oxygen-evolving photosystem II from *Synechococcus vulcanus*, Biochemistry 39 (2000) 14739–14744.
[23] M. Kawamoto, Y. Kawano, N. Kamiya, The bio-crystallography beamline (BL41XU) at SPring-8, Nucl. Instrum. Methods A 467–468 (2001) 1375–1379.
[24] Z. Otwinowski, M. Minor, Processing of x-ray diffraction data collected in oscillation mode, Methods Enzymol. 276 (part A) (1997) 307–326.
[25] COLLABORATIVE COMPUTATIONAL PROJECT, NUMBER 4, The CCP4 Suite: programs for protein crystallography, Acta Cryst. D. 50 (1994) 760–763.
[26] A.T. Brunger, P.D. Adams, G.M. Clore, W.L. DeLano, P. Gros, R.W. Grosse-Kunstleve, J.S. Jiang, I.J. Kuszewsk, M. Nilges, N.S. Pannu, R.J. Read, L.M. Rice, T. Simonson, G.L. Warren, Crystallography & NMR system: a new software suite for macromolecular structure determination, Acta Cryst. D. 54 (1998) 905–921.
[27] H. Kühl, J. Kruip, A. Seidler, A. Krieger-Liszkay, M. Bunker, D. Bald, A.J. Scheidig, M. Rögner, Towards structural determination of the water-splitting enzyme. Purification, crystallization, and preliminary crystallographic studies of photosystem II from a thermophilic cyanobacterium, J. Biol. Chem. 275 (2000) 20652–20659.
[28] E. Haag, K.-D. Irrgang, E.J. Boekema, G. Renger, Functional and structural analysis of photosystem II core complexes from spinach with high oxygen evolution capacity, Eur. J. Biochem. 189 (1990) 47–53.
[29] T. Suzuki, J. Minagawa, T. Tomo, K. Sonoike, H. Ohta, I. Enami, Binding and functional properties of the extrinsic proteins in oxygen-evolving photosystem II particle from a green alga, *Chlamydomonas reinhardtii* having his-tagged CP47, Plant Cell Physiol. 44 (2003) 76–84.
[30] T. Suzuki, O. Tada, M. Makimura, A. Tohri, H. Ohta, Y. Yamamoto, I. Enami, Isolation and characterization of oxygen-evolving photosystem II complexes retaining the PsbO, P and Q proteins from *Euglena gracilis*, Plant Cell Physiol. 45 (2004) 1168–1175.
[31] R. Nagao, A. Ishii, O. Tada, T. Suzuki, N. Dohmae, A. Okumura, M. Iwai, T. Takahashi, Y. Kashino, I. Enami, Isolation and characterization of oxygen-evolving thylakoid membranes and photosystem II particles from a marine diatom *Chaetoceros gracilis*, Biochim. Biophys. Acta 1767 (2007) 1353–1362.
[32] M. Cullen, N. Ray, S. Husain, J. Nugent, J. Nield, S. Purton, A highly active histidine-tagged *Chlamydomonas reinhardtii* photosystem II preparation for structural and biophysical analysis, Photochem. Photobiol. Sci. 6 (2007) 1177–1183.
[33] J. Kern, B. Loll, C. Lüneberg, D. DiFiore, J. Biesiadka, K.D. Irrgang, A. Zouni, Purification, characterisation and crystallisation of photosystem II from *Thermosynechococcus elongatus* cultivated in a new type of photobioreactor, Biochim. Biophys. Acta 1706 (2005) 147–157.
[34] A. Amunts, O. Drory, N. Nelson, The structure of a plant photosystem I supercomplex at 3.4 Å resolution, Nature 447 (2007) 58–63.
[35] M.W. Bowler, M.G. Montgomery, A.G. Leslie, J.E. Walker, Reproducible improvements in order and diffraction limit of crystals of bovine mitochondrial F(1)-ATPase by controlled dehydration, Acta Crystallogr. D. Biol. Crystallogr. 62 (2006) 991–995.